Supporting Information

Validating the arrhythmogenic potential of high, intermediate, and low risk drugs in a human induced pluripotent stem cell (hiPSC)-derived cardiac microphysiological system

Verena Charwat[1‡], Bérénice Charrez[1‡], Brian A. Siemons[1], Henrik Finsberg[2], Karoline H. Jæger[2], Andrew G. Edwards[2], Nathaniel Huebsch[1], Samuel Wall[2], Evan Miller[3], Aslak Tveito[2], Kevin E. Healy[1,4]*

1. Department of Bioengineering and California Institute for Quantitative Biosciences (QB3), University of California at Berkeley, Berkeley, California 94720, USA

2. Simula Research Laboratory, 0164 Oslo, Norway

3. Department of Chemistry, University of California at Berkeley, Berkeley, California 94720, USA

4. Department of Materials Science and Engineering, University of California at Berkeley, Berkeley, California 94720, USA

‡ These authors contributed equally.

* corresponding author: kehealy@berkeley.edu

Table of Contents

Supplementary Table S1: Differences in ion channel activity and other elements of the cellular electrophysiological machinery in WTC vs SCVI20 determined by mathematical modeling.[1] (n.s. not significant, * $p < 0.05$, **** $p < 0.0001$)

Parameter	Current	Cell line with higher activity	Significance level
potassium current	I_{Kr} (hERG)	WTC	*
potassium current	I_{K1}	very similar	n.s.
sodium current	I_{Na}	very similar	n.s.
calcium current	I_{Ca}	very similar	n.s.
Sodium-calcium exchange current	I_{NaCaX}	SCVI20	n.s.
calcium buffer		WTC	****
Ryanodine-receptor flux (RyR)		very similar	n.s.
Intracellular calcium diffusion		very similar	n.s.
SERCA pump activity		WTC	*

Supplementary Table S2: Inter- and intra-batch variation of key electrophysiological parameters in WTC and SCVI20 cell line. A batch refers to a set of tissues loaded at the same time. Different batches were loaded from independent differentiations.

	WTC		**SCVI20**	
	variation within batch	**batch-to-batch variation**	**variation within batch**	**batch-to-batch variation**
beat rate	22%	28%	27%	15%
$cAPD_{80}$	16%	19%	17%	19%
triangulation	17%	23%	22%	9%

Supplementary Table S3: Drug properties.

Drug name	Formulation	CAS-Nr	Company	Product Nr.	MW (g/mol)	TdP risk
Dofetilide	Dofetilide	115256-11-6	ApexBio	A8417	441.56	high
Bepridil	Bepridil hydrochloride	74764-40-2	Sigma-Aldrich	B5016	403	high
Amiodarone	Amiodarone hydrochloride	19774-82-4	Spectrum Chemical	A3972	681.78	intermediate
Terfenadine	Terfenadine	50679-08-8	Sigma-Aldrich	T9652	471.67	intermediate
Nifedipine	Nifedipine	21829-25-4	Sigma-Aldrich	N7634	246.34	low
Mexiletine	Mexiletine hydrochloride	1/4/70	TCI	M2040	215.72	low
Lidocaine	Lidocaine	137-58-6	TCI	L0156	234.34	low

Supplementary Table S4: Drug dose preparation.

Drug	Cmax (μM)	stock (mM)	solvent	final solvent conc	Stock storage	Dose unit	Dose 1	Dose 2	Dose 3	Dose 4	Dose 5
Dofetilide	0.002 [6]	10	DMSO	0.1%	-20°C few months	μM xCmax	0.0001 0.05	0.001 0.5	0.01 5	0.1 50	1 500
Bepridil	0.032 [6]	32	DMSO	0.1%	fresh	μM xCmax	0.0032 0.1	0.032 1	0.32 10	3.2 100	32 1,000
Amiodarone	0.0008 [5]	10	DMSO	0.1%	fresh	μM xCmax	0.001 1.25	0.01 12.5	0.1 125	1 1250	
Terfenadine	0.00028 [6]	3	Ethanol	0.1%	fresh	μM xCmax	0.0003 1	0.003 10	0.03 100	0.3 1,000	3 10,000
Nifedipine	0.0077 [6]	20	DMSO	0.05%	fresh	μM xCmax	0.001 0.125	0.01 1.25	0.1 12.5	1 125	10 1250
Mexiletine	2.5 [6]	50	media	n.a.	fresh	μM xCmax	1 0.4	10 4	100 40	1,000 400	
Lidocaine	2.5 [5]	15	media	n.a.	fresh	μM xCmax	1 0.4	10 4	100 40	1,000 400	

Supplementary Table S5: Ion channel targets.

Drug	**Dofetilide**	**Bepridil**	**Amiodarone**	**Terfenadine**	**Nifedipine**	**Mexiletine**	**Lidocaine**
main target	I_{Kr}	I_{Kr}	I_{Kr}	I_{Kr}	I_{CaL}	I_{NaL}	I_{NaL}
>50% block at highest dose		I_{CaL}, I_{NaL}, I_{Na}		I_{CaL}, I_{NaL}, I_{Na}		I_{Kr}, I_{CaL} , I_{Na}	
15-50% block at highest dose			I_{CaL}				

Supplementary Table S6: Block percentages for drug doses based on drug characteristics from literature.[2-4]

Drug	Dose	Block I_{Kr} (%)	Block I_{CaL} (%)	Block I_{Na} (%)	Block I_{NaL} (%)
Dofetilide [2]	0.1 nM	0.1	0	0	0
	1 nM	1.7	0	0	0
	10 nM	21	0	0	0
	100 nM	80.5	0.2	0	0
	1000 nM	98	2	0.1	0.1
Bepridil [2]	0.0032 µM	2.7	0.1	0	0
	0.032 µM	16.9	1.2	0.5	0.5
	0.32 µM	56	18.1	7.7	7.7
	3.2 µM	80.6	78.1	60.3	60.3
	32 µM	85.6	94.6	96.5	96.5
Amiodarone [2]	1 nM	0.1	0.3	0	0
	10 nM	0.6	1.5	0.1	0.1
	100 nM	7.2	6.6	0.6	0.6
	1000 nM	44.3	22.4	5.5	5.5
Terfenadine [2]	0.3 nM	0.2	0	0	0
	3 nM	3.2	0	0	0
	30 nM	30.2	0.2	0	0
	300 nM	75	11.3	3.1	3.1
	3000 nM	83.8	87.4	66.9	66.9
Nifedipine [2]	0.003 µM	0	17.3	0	0
	0.03 µM	0.2	63.4	0.2	0.2
	0.3 µM	1.2	85.1	0.9	0.9
	3 µM	6.9	88	4.5	4.5
Mexiletine [2, 3]	1 µM	2	1	2.3	4.4
	10 µM	16.7	9.1	18.9	53.8
	100 µM	66.7	50	69.9	96.7
	1000 µM	95.2	90.9	95.8	99.9
Lidocaine [4].	1 µM	0	0	0	4.3
	10 µM	0	0	0	47.5
	100 µM	0	0	0	94.7
	1000 µM	0	0	0	99.7

Supplementary Table S7: IC50 values reported in different studies.

Drug	IC50		
	I_{Kr}	I_{CaL}	I_{Na}
Dofetilide	1 nM [2]	26,700 nM [4]	162,100 nM [4]
	5 nM [3]	60,000 nM [3]	300,000 nM [3]
	7.3-13 nM [5]		
	30 nM [4]		
	70 nM [6]		
Bepridil	0.033 μM [3]	0.211 μM [3]	2.3 μM [4]
	0.149 μM [2]	1.0 μM [4]	2.929 μM [2]
	0.16 μM [4]	2.808 μM [2]	3.7 μM [3]
Amiodarone	30 nM [3]	270 nM [3]	4,577 nM [2]
	860 nM [4]	1,281 nM [2]	4,800 μM [3]
	940 nM [2]	1,900 nM [4]	15,900 μM [4]
Terfenadine	8.9 nM [3]	375 nM [3]	950 nM [6]
	10-18 nM [7]	700 nM [2]	971 nM [3]
	19 nM [2]	930 nM [4]	2,000 nM [4]
	38 nM [6]		
	50 nM [4]		
	54.3-165.4 nM [5]		
Nifedipine	44,000 nM [4]	12 nM [4]	37,000 nM [3]
	275,000 nM [3]	38 nM [8]	88,300 nM [4]
		39 nM [9]	
		60 nM [3]	
Mexiletine	21.4 μM [6]	100 μM [3]	7.6 μM [6]
	50 μM [3]		43 μM [3]

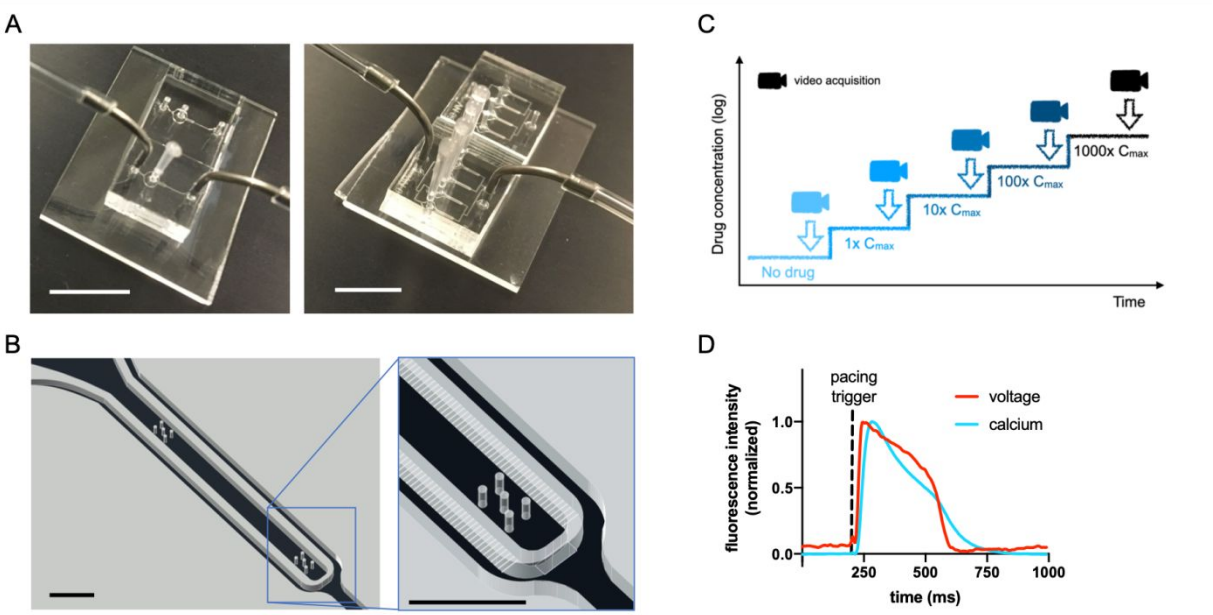

Supplementary Figure S8: Cardiac MPS and experimental plan. A) Photographs of the microfluidic devices show the cardiac MPS with a single tissue chamber (left image) and multiplexed MPS with 4 parallel tissue chambers (right image). Two independent microfluidic systems are bonded to each glass slide. The multiplexed cardiac MPS has plugged cell loading inlets and tubing for media perfusion linked to metal connectors that also serve as pacing electrodes (left image). Scale bars represent approximately 1cm. **B**) AutoCAD rendering of the cardiac MPS showing a cell chamber with 2 sets of anchor pillars (left) and at higher magnification (right) highlighting chamber details such as fenestration that connect the cell chamber to the media channels and weir for cell loading. Scale bars represent 200µm. **C**) Schematic plan of a dose escalation drug study. The same MPS was sequentially exposed to increasing doses of a drug. Initially, no drug was applied, then the first drug dose (range: 0.05-fold to 1.25-fold C_{max}) was perfused followed by 10-fold dose increments. Each dose was incubated for 30min. At the end of the incubation period videos were acquired to record changes in beat waveforms. **D**) Intensity traces were obtained from voltage (red; BeRST-1 dye) and calcium (cyan; GCaMP or OGB-1-AM dye) fluorescence videos. For externally paced samples, the pacing trigger pulse was used to align voltage and calcium traces.

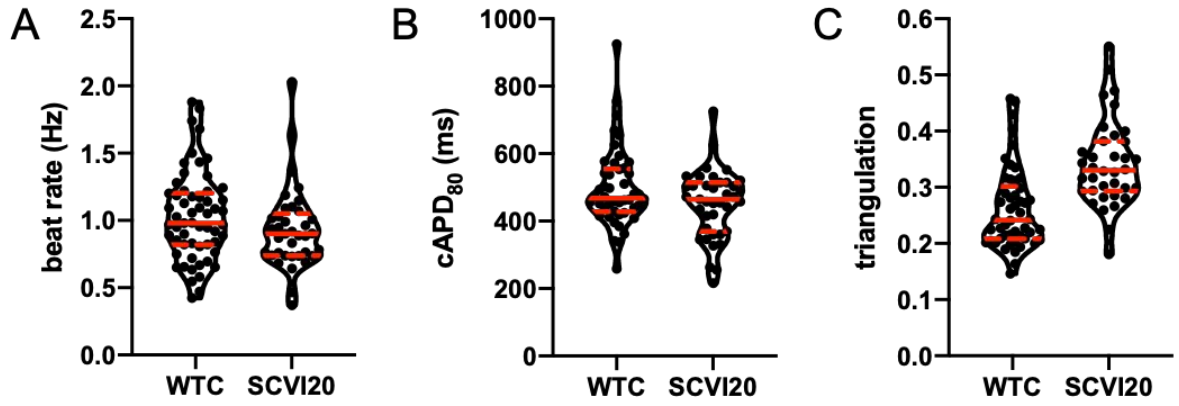

Supplementary Figure S9: Baseline characterization of WTC and SCVI20 MPS. Violin scatter plots of **A**) spontaneous beat rates (WTC 1.03±0.33 Hz; SCVI20 0.93±0.30 Hz), **B**) action potential duration APD_{80} at 1Hz or beat rate corrected to 1Hz (WTC 497±117 ms; SCVI20 451±101 ms), **C**) triangulation calculated as $(APD_{80} - APD_{30})/APD_{80}$ (WTC 0.262±0.072; SCVI20 0.342±0.077). Median and quartiles are indicated in red.

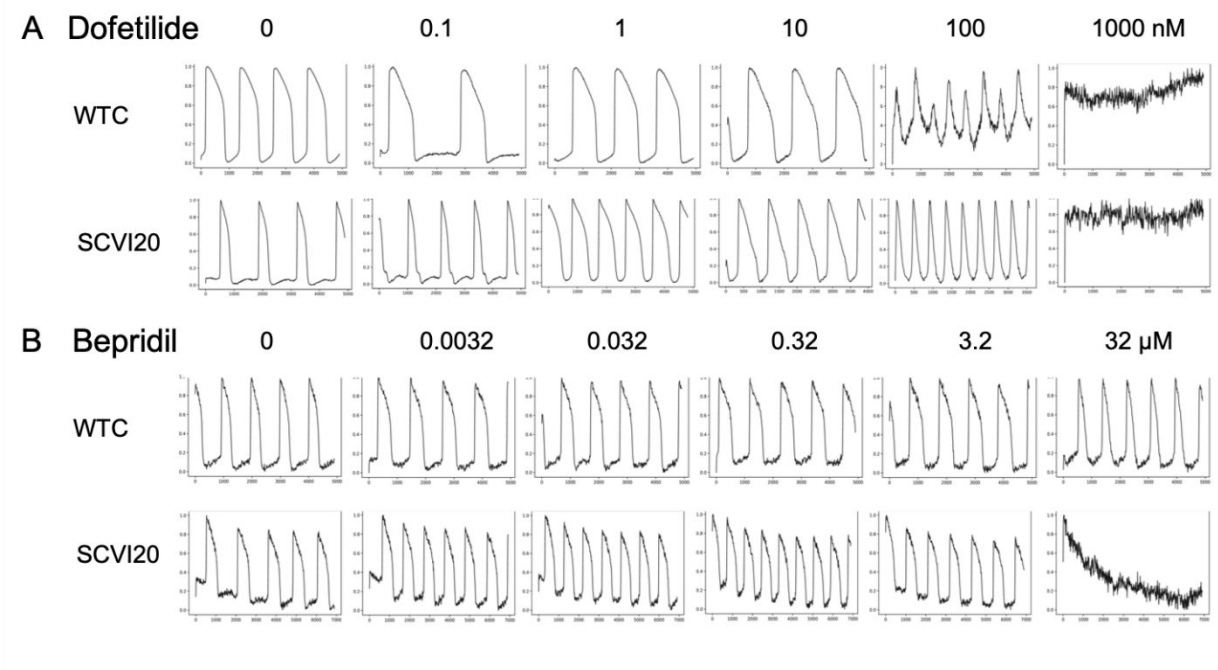

Supplementary Figure S10: Representative voltage traces for high-risk drugs. Voltage traces from MPS exposed to increasing doses of Dofetilide (**A**) or Bepridil (**B**). Representative traces are shown for a WTC tissue (top row) and a SCVI20 tissue (bottom row) after background subtraction and normalization to the intensity range 0 to 1.

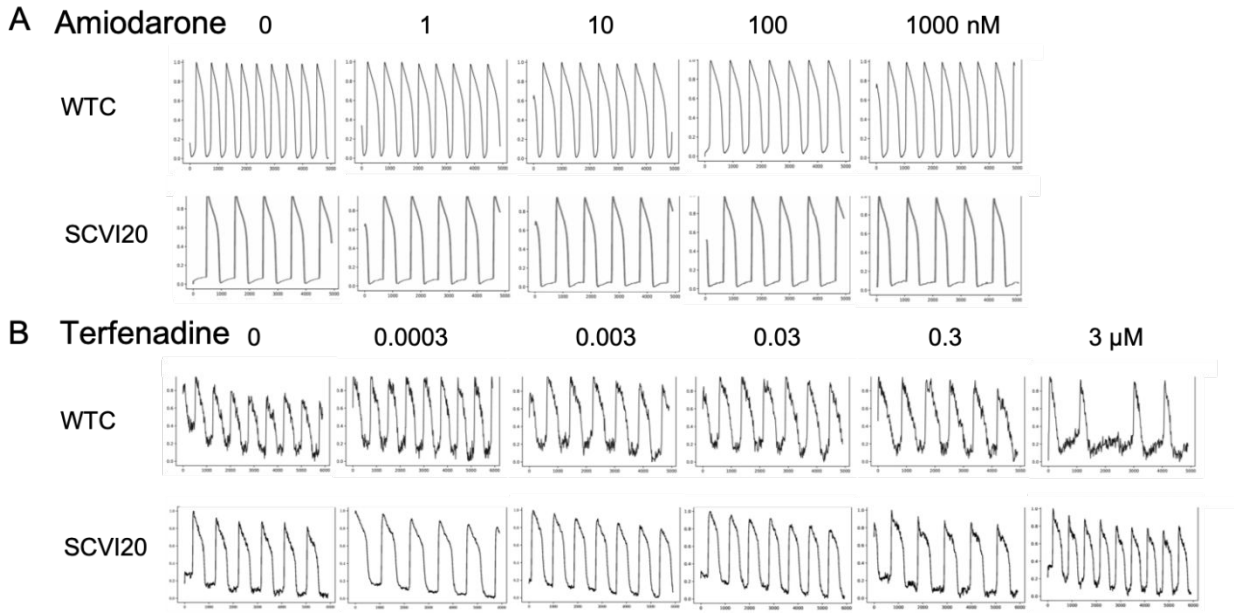

Supplementary Figure S11: Representative voltage traces for intermediate-risk drugs. Voltage traces from MPS exposed to increasing doses of Amiodarone (**A**) or Terfenadine (**B**). Representative traces are shown for a WTC tissue (top row) and a SCVI20 tissue (bottom row) after background subtraction and normalization to the intensity range 0 to 1.

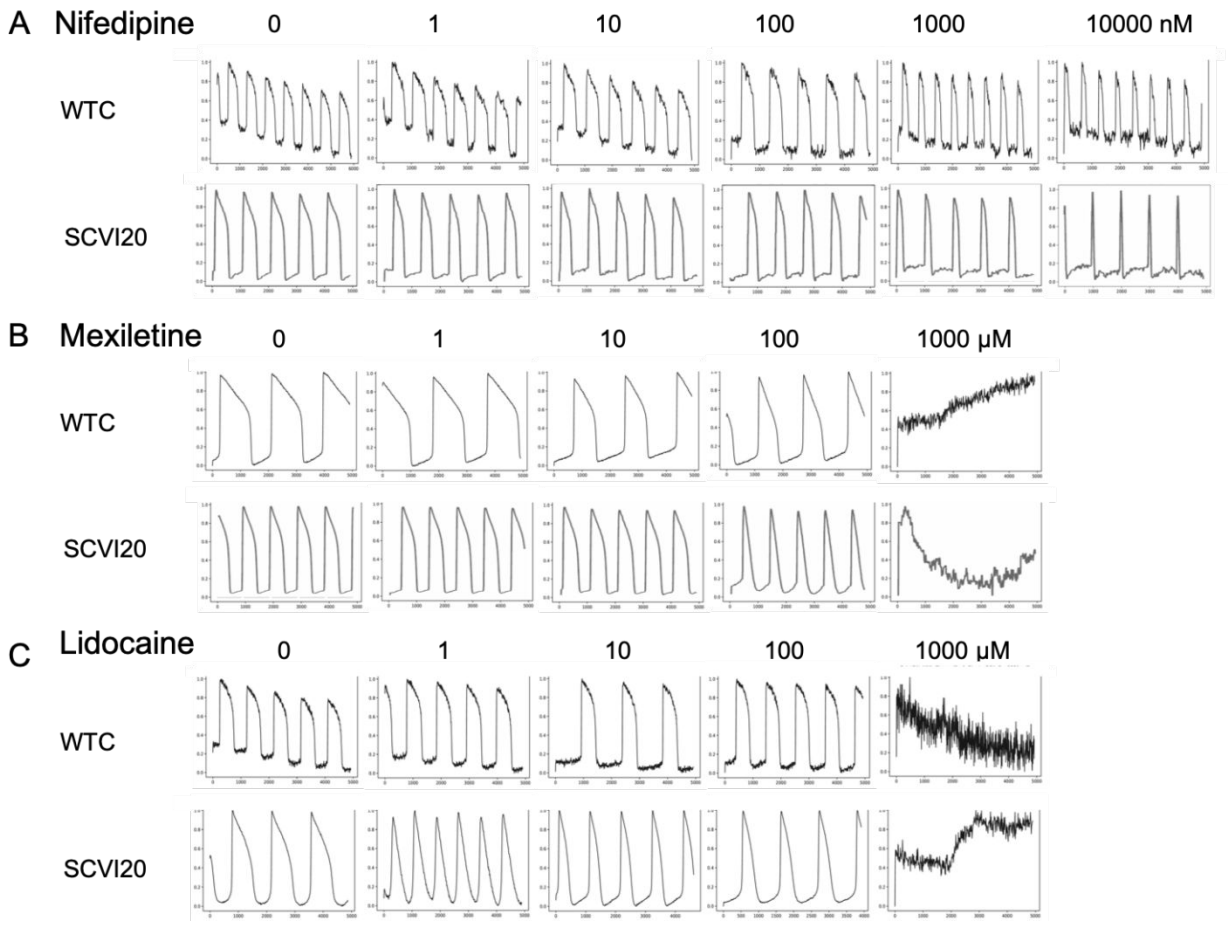

Supplementary Figure S12: Representative voltage traces for low-risk drugs. Voltage traces from MPS exposed to increasing doses of Nifedipine (**A**), Mexiletine (**B**) or Lidocaine (**C**). Representative traces are shown for a WTC tissue (top row) and a SCVI20 tissue (bottom row) after background subtraction and normalization to the intensity range 0 to 1.

References

(1) Huebsch, N.; Charrez, B.; Neiman, G.; Siemons, B.; Boggess, S. C.; Wall, S.; Charwat, V.; Jæger, K. H.; Cleres, D.; Telle, Å.; et al. Metabolically driven maturation of human-induced-pluripotent-stem-cell-derived cardiac microtissues on microfluidic chips. *Nat Biomed Eng* **2022**, *6* (4), 372-388. DOI: 10.1038/s41551-022-00884-4.
(2) Crumb, W. J.; Vicente, J.; Johannesen, L.; Strauss, D. G. An evaluation of 30 clinical drugs against the comprehensive in vitro proarrhythmia assay (CiPA) proposed ion channel panel. *J Pharmacol Toxicol Methods* **2016**, *81*, 251-262. DOI: 10.1016/j.vascn.2016.03.009.
(3) Mirams, G. R.; Cui, Y.; Sher, A.; Fink, M.; Cooper, J.; Heath, B. M.; McMahon, N. C.; Gavaghan, D. J.; Noble, D. Simulation of multiple ion channel block provides improved early prediction of compounds' clinical torsadogenic risk. *Cardiovasc Res* **2011**, *91* (1), 53-61. DOI: 10.1093/cvr/cvr044.
(4) Kramer, J.; Obejero-Paz, C. A.; Myatt, G.; Kuryshev, Y. A.; Bruening-Wright, A.; Verducci, J. S.; Brown, A. M. MICE models: superior to the HERG model in predicting Torsade de Pointes. *Sci Rep* **2013**, *3*, 2100. DOI: 10.1038/srep02100.
(5) Orvos, P.; Kohajda, Z.; Szlovák, J.; Gazdag, P.; Árpádffy-Lovas, T.; Tóth, D.; Geramipour, A.; Tálosi, L.; Jost, N.; Varró, A.; et al. Evaluation of Possible Proarrhythmic Potency: Comparison of the Effect of Dofetilide, Cisapride, Sotalol, Terfenadine, and Verapamil on hERG and Native IKr Currents and on Cardiac Action Potential. *Toxicol Sci* **2019**, *168* (2), 365-380. DOI: 10.1093/toxsci/kfy299.
(6) Qu, Y.; Vargas, H. M. Proarrhythmia Risk Assessment in Human Induced Pluripotent Stem Cell-Derived Cardiomyocytes Using the Maestro MEA Platform. *Toxicol Sci* **2015**, *147* (1), 286-295. DOI: 10.1093/toxsci/kfv128.
(7) Katayama, Y.; Tsuzaki, T.; Abe, K.; Tomizawa, S.; Izumi, T.; Tsurubuchi, Y. The inter-cell-line reproducibility of hERG assay using the whole-cell patch-clamping. *J. Pharmacol. Sci.* **2005**, *97*.
(8) Ma, J.; Guo, L.; Fiene, S. J.; Anson, B. D.; Thomson, J. A.; Kamp, T. J.; Kolaja, K. L.; Swanson, B. J.; January, C. T. High purity human-induced pluripotent stem cell-derived cardiomyocytes: electrophysiological properties of action potentials and ionic currents. *Am J Physiol Heart Circ Physiol* **2011**, *301* (5), H2006-2017. DOI: 10.1152/ajpheart.00694.2011.
(9) Gibson, J. K.; Yue, Y.; Bronson, J.; Palmer, C.; Numann, R. Human stem cell-derived cardiomyocytes detect drug-mediated changes in action potentials and ion currents. *J Pharmacol Toxicol Methods* **2014**, *70* (3), 255-267. DOI: 10.1016/j.vascn.2014.09.005.